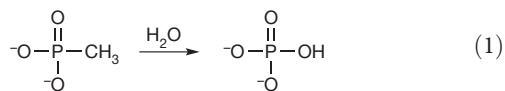


# Intermediates in the transformation of phosphonates to phosphate by bacteria

Siddhesh S. Kamat<sup>1</sup>, Howard J. Williams<sup>1</sup> & Frank M. Raushel<sup>1</sup>

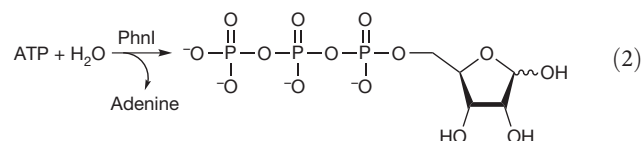
Phosphorus is an essential element for all known forms of life. In living systems, phosphorus is an integral component of nucleic acids, carbohydrates and phospholipids, where it is incorporated as a derivative of phosphate. However, most Gram-negative bacteria have the capability to use phosphonates as a nutritional source of phosphorus under conditions of phosphate starvation<sup>1</sup>. In these organisms, methylphosphonate is converted to phosphate and methane. In a formal sense, this transformation is a hydrolytic cleavage of a carbon–phosphorus (C–P) bond, but a general enzymatic mechanism for the activation and conversion of alkylphosphonates to phosphate and an alkane has not been elucidated despite much effort for more than two decades. The actual mechanism for C–P bond cleavage is likely to be a radical-based transformation<sup>2</sup>. In *Escherichia coli*, the catalytic machinery for the C–P lyase reaction has been localized to the *phn* gene cluster<sup>1</sup>. This operon consists of the 14 genes *phnC*, *phnD*, ..., *phnP*. Genetic and biochemical experiments have demonstrated that the genes *phnG*, *phnH*, ..., *phnM* encode proteins that are essential for the conversion of phosphonates to phosphate and that the proteins encoded by the other genes in the operon have auxiliary functions<sup>1,3–6</sup>. There are no functional annotations for any of the seven proteins considered essential for C–P bond cleavage. Here we show that methylphosphonate reacts with MgATP to form  $\alpha$ -D-ribose-1-methylphosphonate-5-triphosphate (RPnTP) and adenine. The triphosphate moiety of RPnTP is hydrolysed to pyrophosphate and  $\alpha$ -D-ribose-1-methylphosphonate-5-phosphate (PRPn). The C–P bond of PRPn is subsequently cleaved in a radical-based reaction producing  $\alpha$ -D-ribose-1,2-cyclic-phosphate-5-phosphate and methane in the presence of *S*-adenosyl-L-methionine. Substantial quantities of phosphonates are produced worldwide for industrial processes, detergents, herbicides and pharmaceuticals<sup>7–9</sup>. Our elucidation of the chemical steps for the biodegradation of alkylphosphonates shows how these compounds can be metabolized and recycled to phosphate.

The bacterial C–P lyase gene cluster enables alkylphosphonates to be converted to phosphate (equation (1)).

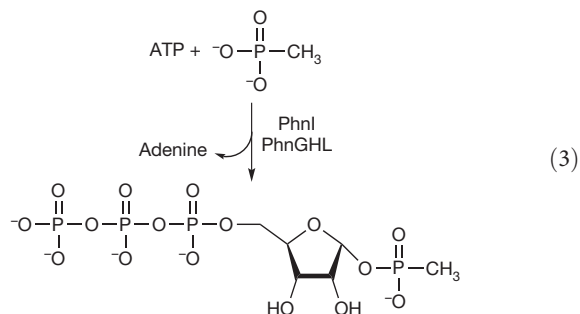


We cloned the genes *phnG*, *phnH*, ..., *phnM* and expressed them in *E. coli*, and purified to homogeneity the resulting proteins. PhnI, PhnJ, PhnK and PhnL were purified as amino-terminal glutathione S-transferase (GST) fusion proteins. PhnG, PhnH and PhnM were purified without a GST tag. Previous experiments have hinted that a ribose intermediate exists in the esterification of phosphonate substrates before conversion to phosphate<sup>10,11</sup>. Because PhnI showed a distant relationship to enzymes that are functionally annotated as nucleosidases<sup>12</sup>, we incubated this protein with a small, focused library of potential ribose donors. The liberation of the free base was followed spectrophotometrically at 240–350 nm in the presence of coupling enzymes that are capable of detecting the formation of adenine<sup>13</sup>,

guanine<sup>14</sup>, cytosine<sup>15</sup> or xanthine<sup>16</sup>. The best substrates for PhnI are GTP ( $k_{\text{cat}}/K_{\text{m}} = 8.3 \times 10^4 \text{ M}^{-1} \text{ s}^{-1}$ ;  $k_{\text{cat}}$ , turnover number;  $K_{\text{m}}$ , Michaelis constant) and ATP ( $k_{\text{cat}}/K_{\text{m}} = 1.3 \times 10^4 \text{ M}^{-1} \text{ s}^{-1}$ ). The products are D-ribose-5-triphosphate (RTP) and the free base as shown for ATP in equation (2). The kinetic constants for the nucleosidase activity of PhnI with GTP and ATP are listed in Supplementary Table 1. The structure of RTP was identified by <sup>31</sup>P NMR spectroscopy and further confirmed by multidimensional NMR.



The formation of RTP from either ATP or GTP did not seem to be a productive pathway for the transformation of phosphonates to phosphate. We therefore incubated phosphate and phosphonate derivatives with MgATP in the presence of PhnI to determine whether any of these compounds could displace adenine. RTP and adenine were the only products formed in the presence of either phosphate or phosphonate derivatives. There were no changes in the reaction products when we used the GST-tagged PhnI in the presence or absence of factor Xa<sup>17</sup>. Because it was previously postulated that the C–P lyase reaction may involve a multiprotein complex<sup>3,18</sup>, we added additional proteins to the reaction mixture. PhnG, PhnH, PhnK and PhnL were incubated together with PhnI, MgATP and methylphosphonate, but no new products were detected. Because PhnI, PhnK and PhnL were all present as GST fusion proteins, factor Xa was added to the reaction mixture for *in situ* cleavage of the GST tags. After addition of factor Xa, a new resonance was observed by <sup>31</sup>P NMR spectroscopy at a chemical shift of 17.8 p.p.m. (Fig. 1a). The NMR spectra are consistent with the formation of RPnTP, shown in equation (3).



To determine whether all of the proteins are required for this transformation, we removed each protein individually from the reaction mixture. The only protein that could be removed without affecting the transformation was PhnK. Thus, PhnI, in the presence of PhnG, PhnH and PhnL, is required to catalyse the nucleophilic attack of methylphosphonate on the anomeric carbon of MgATP to form adenine and RPnTP. The kinetic constants for the reaction of methylphosphonate with ATP ( $k_{\text{cat}}/K_{\text{m}} = 3.5 \times 10^5 \text{ M}^{-1} \text{ s}^{-1}$ ) and GTP ( $k_{\text{cat}}/K_{\text{m}} = 3.4 \times 10^5 \text{ M}^{-1} \text{ s}^{-1}$ ) in the presence of PhnI, PhnG, PhnH and

<sup>1</sup>Department of Chemistry, PO Box 30012, Texas A&M University, College Station, Texas 77843, USA.

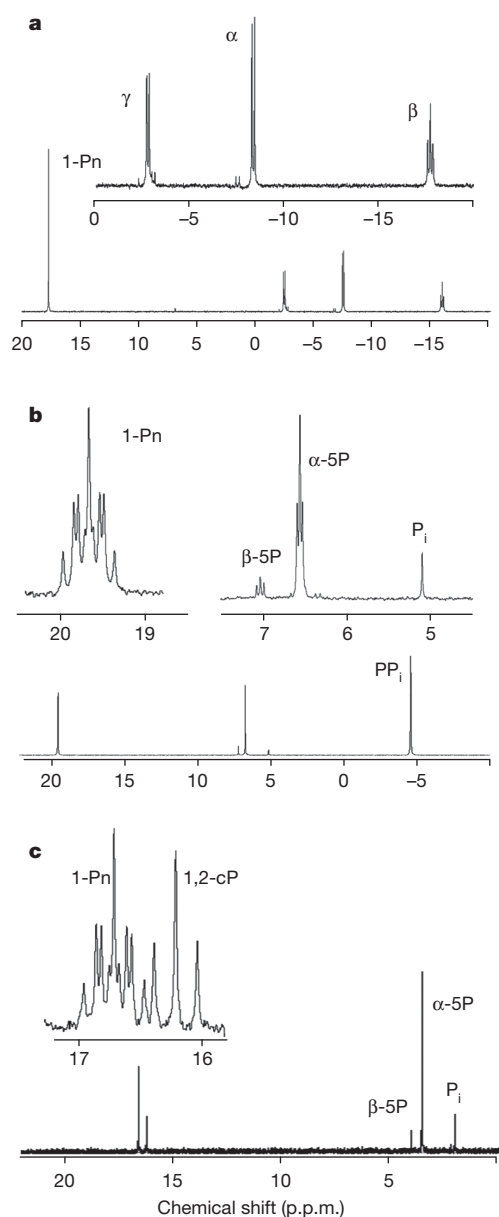
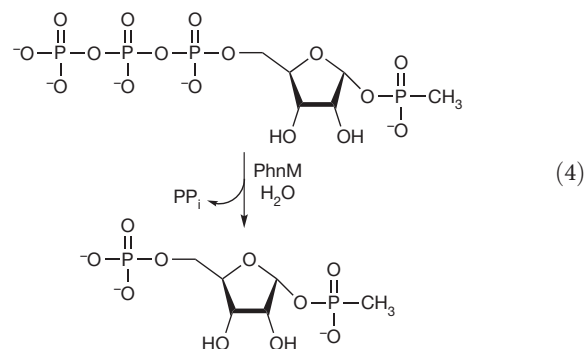


**Figure 1**  $^{31}\text{P}$  NMR spectra of the reaction products catalysed by PhnI, PhnM and PhnJ. **a**, RPNTP from the reaction of methylphosphonate and MgATP catalysed by PhnI in the presence of PhnG, PhnH, and PhnL at pH 8.5. The methylphosphonyl group is labelled as 1-Pn. Inset,  $^{31}\text{P}$ – $^{31}\text{P}$  coupling of the triphosphate portion of the RPNTP product (the  $\alpha$ ,  $\beta$  and  $\gamma$  phosphoryl groups). **b**, The formation of PRPN from RPNTP in the presence of PhnM. Inset, proton-coupled spectrum at pH 8.5 showing the multiplet that corresponds to 1-Pn and the triplet that corresponds to the 5-phosphate (5P).  $\text{P}_i$ , inorganic phosphate. **c**, The formation of PRcP from PRPN in the presence of PhnJ at pH 6.8. Inset, proton-coupled spectrum showing the formation of a new triplet that corresponds to the 1,2-cyclic moiety of PRcP (1,2-cP). The chemical shifts for the phosphate moiety at the fifth carbon atom of PRcP and PRPN are coincident with one another (3.4 p.p.m.).

PhnL are presented in Supplementary Table 1. We note that these proteins begin to precipitate after removal of the GST tags and that the kinetic constants are therefore not definitive. No reaction was observed with the fusion proteins, and the GST tags must be removed *in situ*. The stoichiometries of the four proteins required for complex formation and the individual functions of PhnG, PhnH and PhnL are uncertain.

Previous studies have suggested that PRPN is a potential intermediate in the conversion of alkylphosphonates to phosphate by *E. coli*<sup>6,10,11</sup>.

Hence, it was rational to assume that one of the proteins expressed by the *phn* operon would catalyse the hydrolysis of the  $\beta$ - and  $\gamma$ -phosphoryl groups from RPNTP. PhnM is the prime candidate for this reaction because this protein is a member of the amidohydrolase superfamily, members of which are known to catalyse hydrolytic reactions at carbon and phosphorus centres<sup>19</sup>. We incubated PhnM with RPNTP in the presence of  $\text{MgCl}_2$  and  $\text{ZnCl}_2$ . The changes in the  $^{31}\text{P}$  NMR spectrum are shown in Fig. 1b. The NMR spectra are consistent with the formation of PRPN and pyrophosphate as the major products. D-ribose-5-diphosphate and RTP are also substrates for PhnM. When the hydrolysis reaction of RTP catalysed by PhnM was conducted in  $^{18}\text{O}$ -labelled water, the  $^{18}\text{O}$  was found exclusively in D-ribose-5-phosphate and not in pyrophosphate. Therefore, water attacks the  $\alpha$ -phosphoryl group of RTP rather than the  $\beta$ -phosphoryl group. The reaction catalysed by PhnM with RPNTP is presented in equation (4). The kinetic constants for the hydrolysis of RPNTP, RTP and D-ribose-5-diphosphate by PhnM are provided in Supplementary Table 1. RPNTP ( $k_{\text{cat}}/K_m = 1.1 \times 10^5 \text{ M}^{-1} \text{ s}^{-1}$ ) was the best substrate for PhnM and the kinetic constants did not change for the hydrolysis of RPNTP when PhnG, PhnH, PhnI, PhnK, PhnL and factor Xa were added to the assay mixture.



The deletion of *phnJ* from *E. coli* led to the identification of  $\alpha$ -D-ribose-1-methylphosphonate in the growth medium, and this led to the prediction that PRPN is the ultimate substrate for the C–P lyase reaction<sup>6</sup>. This conjecture is consistent with our results because we can synthesize PRPN from ATP and methylphosphonate by the combined actions of PhnI, PhnG, PhnH, PhnL and PhnM. Of the remaining two enzymes expressed by the *phn* operon, the protein most likely to catalyse the C–P bond cleavage is PhnJ. This enzyme has four conserved cysteine residues, with a spacing of  $\text{CX}_2\text{CX}_{21}\text{CX}_5\text{C}$  (where  $\text{X}_n$  denotes a sequence of some  $n$  amino acids), that could form part of an iron–sulphur (Fe–S) cluster<sup>12</sup>. The cleavage of PRPN to  $\alpha$ -D-ribose-1,2-cyclic-phosphate-5-phosphate (PRcP) is assumed to involve a radical mechanism and such reactions can be catalysed by radical SAM enzymes. These enzymes use a [4Fe–4S] cluster and S-adenosyl-L-methionine (SAM) to catalyse radical reactions and/or rearrangements<sup>20</sup>. The radical SAM superfamily was originally thought to have a highly conserved  $\text{CX}_3\text{CX}_2\text{C}$  motif as a signature for harbouring the [4Fe–4S] cluster<sup>20</sup>, but with the successful reconstitutions of ThiC<sup>21</sup>, HmdA<sup>22</sup> and Dph2<sup>23</sup> a more diverse combination of conserved cysteine residues can function for the assembly of the [4Fe–4S] cluster. If PhnJ incorporates a [4Fe–4S] cluster, it is not clear which of the four cysteine residues are required.

The as-purified GST–PhnJ fusion protein was blackish in colour. Inductively coupled plasma mass spectroscopy of this protein demonstrated the binding of  $2.2 \pm 0.2$  equiv. of iron per PhnJ monomer. The aerobically purified protein was made anaerobic in a glove box by bubbling argon through the protein solution and then allowed it to equilibrate for 4 h. Reconstitution of the [4Fe–4S] cluster was initiated by the slow anaerobic addition of a 50-fold excess of  $\text{FeSO}_4$  and  $\text{Na}_2\text{S}$ . The protein with the reconstituted Fe–S cluster had a reddish-brown colour. The ultraviolet–visible absorption spectrum of PhnJ,

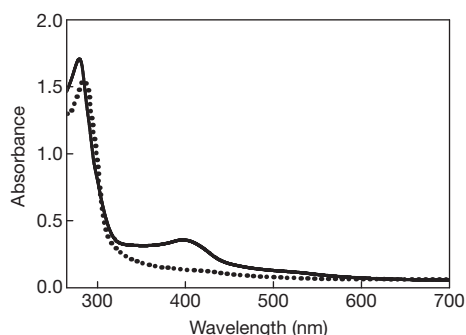
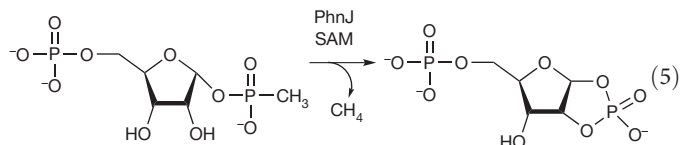


**Figure 2** | Ultraviolet-visible absorbance spectrum of PhnJ (31  $\mu\text{M}$ ) after anaerobic reconstitution of the Fe-S cluster (solid line). The peak at 280 nm is due to the protein and the absorbance centred at 403 nm represents the  $[\text{4Fe-4S}]^{2+}$  cluster. The dotted line represents the absorbance spectrum of PhnJ (27  $\mu\text{M}$ ) reconstituted with a  $[\text{4Fe-4S}]^{2+}$  cluster after reduction of the cluster with sodium dithionite to the  $[\text{4Fe-4S}]^+$  form.

reconstituted with iron and sulphide, had a broad absorption band centred at 403 nm that is indicative of a  $[\text{4Fe-4S}]^{2+}$  cluster<sup>20–23</sup> (Fig. 2). The absorption band disappears on addition of 1 mM dithionite (Fig. 2), suggesting the reduction of the  $[\text{4Fe-4S}]^{2+}$  cluster to the  $[\text{4Fe-4S}]^+$  species, which is the active form for most radical SAM enzymes<sup>20–23</sup>.

There are two compounds that are potential substrates for cleavage by PhnJ of the C–P phosphonate bond: PRPn and RPnTP. Both of these compounds were incubated with 125  $\mu\text{M}$  PhnJ with a  $[\text{4Fe-4S}]$  cluster, 2 mM SAM and 1 mM dithionite, anaerobically, at pH 6.8. We analysed the reactions by  $^{31}\text{P}$  NMR spectroscopy but observed no change in the NMR spectrum for either substrate. When the reaction was supplemented with factor Xa, no change in the  $^{31}\text{P}$  NMR spectrum with RPnTP was observed, but a new resonance appeared at 16.2 p.p.m. when PRPn was used as a substrate (Fig. 1c). The increase in the resonance at 16.2 p.p.m. correlated with a decrease in the phosphonate resonance of PRPn at 16.6 p.p.m. The new resonance splits into a triplet in the  $^1\text{H}$ -coupled  $^{31}\text{P}$  spectrum (Fig. 1c, inset), demonstrating that the product is no longer a methylphosphonate. The new resonance is consistent with a cyclic phosphate, and the proton coupling constant of 21 Hz indicates that the phosphate moiety of the product is esterified to the hydroxyl groups attached to the first

and second carbons atoms of the ribose. Thus, PhnJ requires a reduced  $[\text{4Fe-4S}]$  cluster and SAM to catalyse the formation of PRcP from PRPn. The overall reaction is illustrated in equation (5). There was no reaction in the absence of added SAM.



We used gas chromatography and mass spectrometry to confirm the formation of methane. The  $[\text{4Fe-4S}]$ -cluster-reconstituted PhnJ was incubated with 2 mM SAM, 1 mM dithionite, 5 mM PRPn and factor Xa in a sealed tube for 5 h. Gas chromatographic analysis of the headspace above the liquid showed a single peak that co-eluted with a methane standard (Supplementary Fig. 2). The formation of methane was confirmed by coupling the output of the gas chromatography to a mass spectrometer and detection of a molar mass of  $16\text{ g mol}^{-1}$  (approximately that of methane). Thus, the two products that form from the action of PhnJ on PRPn are methane and PRcP. We were unable to detect the formation of methanol or formaldehyde in the reaction mixture.

The addition of SAM, dithionite, PhnJ and factor Xa were required for the formation of PRcP and methane from the  $[\text{4Fe-4S}]^{2+}$ -cluster-reconstituted PhnJ. To determine the fate of SAM during the reaction, we used high-performance liquid chromatography and amino-acid analysis. Liquid chromatography showed the formation of 5'-deoxyadenosine, and amino-acid analysis confirmed the formation of methionine. These products were formed only when PhnJ (with a reconstituted Fe–S cluster), factor Xa, SAM, dithionite and PRPn were added to the reaction mixture. The omission of any one of the above components resulted in no formation of 5'-deoxyadenosine (Supplementary Fig. 3). The concentration of PRcP and methane formed in the presence of reconstituted PhnJ and SAM showed that one to four turnovers of product were formed per PhnJ monomer. The small number of turnovers per enzyme may reflect the poor solubility of PhnJ after proteolytic cleavage of the N-terminal GST fusion tag and the instability of the  $[\text{4Fe-4S}]$  cluster. A working model for the conversion of PRPn to PRcP by PhnJ is presented in Fig. 3.

The reaction intermediates for the conversion of alkylphosphonates to phosphate in *E. coli* have now been identified. PhnI, in the presence

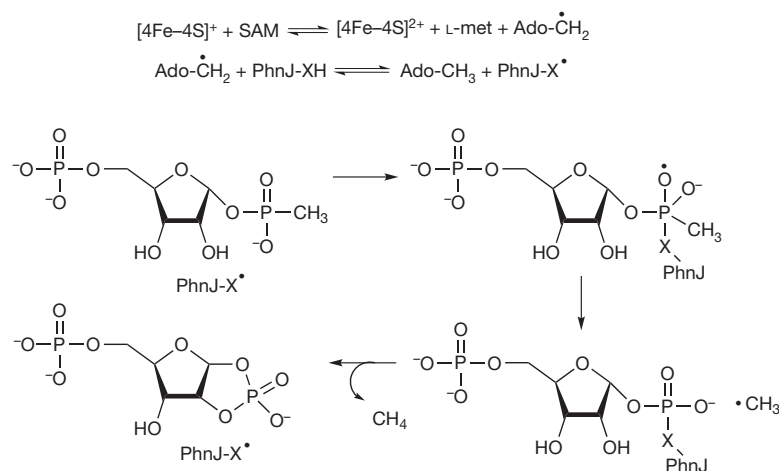


**Figure 3** | Working model for the transformation of PRPn to PRcP. The cleavage of the C–P bond in PRPn by PhnJ reconstituted with a  $[\text{4Fe-4S}]^{1+}$  cluster and SAM is probably initiated by electron transfer from the Fe–S cluster to reductively cleave SAM and thus transiently generate L-methionine (L-met) and a 5'-deoxyadenosyl radical ( $\text{Ado-}\dot{\text{C}}\text{H}_2$ ). This radical may subsequently catalyse the formation of a protein radical ( $\text{PhnJ-X}^\bullet$ ), presumably a cysteine-based thiyl radical. Thiyl radicals have previously been demonstrated in

pyruvate formate lyase<sup>24,25</sup> and methyl coenzyme M reductase<sup>26</sup>. The thiyl radical may attack the phosphonate moiety of the substrate to liberate a methyl radical with formation of a thioester intermediate. Intramolecular attack by the hydroxyl of the second carbon atom of the substrate would generate PRcP and the free thiol group. Methane would be formed through hydrogen atom abstraction from either 5'-deoxyadenosine or the putative cysteine residue.

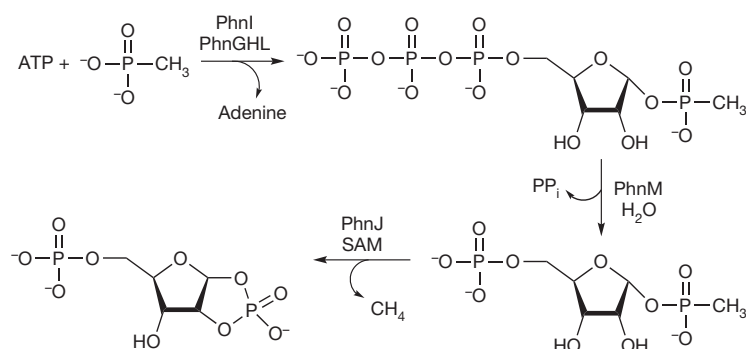


**Figure 4 | Reaction pathway for the conversion of methylphosphonate to PRCp.** The proteins PhnG, PhnH, PhnI, PhnJ, PhnL and PhnM are required for this transformation. The role of PhnK is unknown. PhnGHL denotes PhnG, PhnH and PhnL.

of PhnG, PhnH and PhnL, catalyses the formation of RPNTP from MgATP and methylphosphonate. PhnM catalyses the hydrolysis of RPNTP to pyrophosphate and PRPn. PhnJ can be reconstituted anaerobically with an Fe-S cluster using ferrous sulphate, sodium sulphide and sodium dithionite. The reconstituted PhnJ catalyses the SAM-dependent radical cleavage of the C-P bond of PRPn to form PRCp and methane. The transformations catalysed by the C-P lyase system in *E. coli* are summarized in Fig. 4.

## METHODS SUMMARY

**Protein expression and purification.** All vectors bearing the appropriate genes were transformed in BL21 DE3 cells and inoculated into lysogeny broth medium. Cells were grown at 37 °C to an absorbance of  $A_{600\text{ nm}}$  0.4, after which the temperature was reduced to 18 °C. At  $A_{600\text{ nm}}$  0.6, the cells were induced with 0.5 mM isopropyl- $\beta$ -D-thiogalactoside. Cells were grown for 18–20 h after induction. Overexpression was confirmed by SDS-polyacrylamide gel electrophoresis. Detailed descriptions of the protein purification protocols are presented in Supplementary Information. All GST-tagged proteins (PhnI, PhnJ, PhnK and PhnL) were purified on a GSTrap column (GE Healthcare; 5 ml) and all poly-His tag proteins (PhnG and PhnH) were purified on a HisTrap column (GE Healthcare; 5 ml) following the manufacturer's instructions. PhnM was purified using gel filtration with a High Load Superdex 200 26/60 prep grade column followed by anion exchange chromatography (ResourceQ; 6 ml). The chemical reconstitution of PhnJ is explained in detail in Supplementary Information.

**Purification of reaction products and NMR spectroscopy.** All reactions were filtered by centrifugation through a 10- or 30-kDa membrane (VWR Chemicals) to separate the enzymes from the reaction mixture. The filtrate (0.5 ml) was loaded onto a 1-ml ResourceQ column and eluted with 0.1–1 M ammonium bicarbonate over 20 ml using an AKTA Purifier 10 high-performance liquid chromatograph. The peak fractions were collected and vacuum dried at 4 °C. The products were analysed by <sup>1</sup>H, <sup>13</sup>C and <sup>31</sup>P NMR. The samples for <sup>31</sup>P NMR (D<sub>2</sub>O, 85% H<sub>3</sub>PO<sub>4</sub> corresponds to  $\delta = 0.00$ ) were made in 50 mM HEPES, 10% D<sub>2</sub>O, pH 8.5–8.8 (or pH 6.8 for PhnJ) and analysed with a Varian Unity Inova 500 MHz NMR spectrometer or a Bruker Avance III 400 MHz NMR spectrometer. <sup>1</sup>H and <sup>13</sup>C NMR spectra were acquired on a Bruker Avance III 500 MHz NMR spectrometer equipped with an HCN cryoprobe.

Received 2 May; accepted 10 October 2011.

Published online 16 November 2011.

1. Metcalf, W. W. & Wanner, B. L. Evidence for a fourteen-gene, *phnC* to *phnP* locus for phosphonate metabolism in *Escherichia coli*. *Gene* **129**, 27–32 (1993).
2. Ahn, Y., Ye, Q., Cho, H., Walsh, C. T. & Floss, H. G. Stereochemistry of carbon-phosphorus cleavage in ethylphosphonate catalyzed by C-P lyase from *Escherichia coli*. *J. Am. Chem. Soc.* **114**, 7953–7954 (1992).
3. Metcalf, W. W. & Wanner, B. L. Mutational analysis of an *Escherichia coli* fourteen-gene operon for phosphonate degradation, using TnphoA' elements. *J. Bacteriol.* **175**, 3430–3442 (1993).
4. Hove-Jensen, B., Rosenkrantz, T. J., Haldimann, A. & Wanner, B. L. *Escherichia coli phnN*, encoding ribose 1,5-bisphosphokinase activity (phosphoribosyl diphosphate forming): dual role in phosphonate degradation and NAD biosynthesis pathways. *J. Bacteriol.* **185**, 2793–2801 (2003).
5. Errey, J. C. & Blanchard, J. S. Functional annotation and kinetic characterization of PhnO from *Salmonella enterica*. *Biochemistry* **45**, 3033–3039 (2006).
6. Hove-Jensen, B., McSorley, F. R. & Zechel, D. L. Physiological role of *phnP*-specified phosphoribosyl cyclic phosphodiesterase in catabolism of organophosphoric acids by the carbon-phosphorus lyase pathway. *J. Am. Chem. Soc.* **133**, 3617–3624 (2011).
7. Ternan, N. G., McGrath, J. W., McMullan, G. & Quinn, J. P. Organophosphonates: occurrence, synthesis and biodegradation by microorganisms. *World J. Microbiol. Biotechnol.* **14**, 635–647 (1998).

8. Kononova, S. V. & Nesmeyanova, M. A. Phosphonates and their degradation by microorganisms. *Biochemistry (Mosc.)* **67**, 184–195 (2002).
9. White, A. K. & Metcalf, W. W. Microbial metabolism of reduced phosphorus compounds. *Annu. Rev. Microbiol.* **61**, 379–400 (2007).
10. Avila, L. Z., Draths, K. M. & Frost, J. W. Metabolites associated with organophosphonate C-P bond cleavage: chemical synthesis and microbial degradation of [<sup>32</sup>P]-ethylphosphonic acid. *Bioorg. Med. Chem. Lett.* **1**, 51–54 (1991).
11. Frost, J. W., Loo, S., Cordeiro, M. L. & Li, D. Radical-based dephosphorylation and organophosphonate biodegradation. *J. Am. Chem. Soc.* **109**, 2166–2171 (1987).
12. Parker, G. F., Higgins, T. P., Hawkes, T. & Robson, R. L. *Rhizobium (Sinorhizobium) meliloti phn* genes: characterization and identification of their protein products. *J. Bacteriol.* **181**, 389–395 (1999).
13. Kamat, S. S. *et al.* Catalytic mechanism and three-dimensional structure of adenine deaminase. *Biochemistry* **50**, 1917–1927 (2011).
14. Maynes, J. T., Yuan, R. G. & Snyder, F. F. Identification, expression and characterization of the *Escherichia coli* guanine deaminase. *J. Bacteriol.* **182**, 4658–4660 (2000).
15. Hall, R. S. *et al.* Three dimensional structure and catalytic mechanism of cytosine deaminase. *Biochemistry* **50**, 5077–5085 (2011).
16. Krenitsky, T. A., Neil, S. M., Elion, G. B. & Hitchings, G. H. A comparison of the specificities of xanthine oxidase and aldehyde oxidase. *Arch. Biochem. Biophys.* **150**, 585–599 (1972).
17. La Vallie, E. R., McCoy, J. M., Smith, D. B. & Riggs, P. Enzymatic and chemical cleavage of fusion proteins. *Curr. Protocols Mol. Biol.* Unit 16.4B (1994).
18. Jochimsen, B. *et al.* Five phosphonate operon gene products as components of a multi-enzyme complex of the carbon-phosphorus lyase pathway. *Proc. Natl Acad. Sci. USA* **108**, 11393–11398 (2011).
19. Seibert, C. M., & Raushel, F. M. Structural and catalytic diversity within the amidohydrolase superfamily. *Biochemistry* **44**, 6383–6391 (2005).
20. Frey, P. A., Hegeman, A. D. & Ruzicka, F. J. The radical SAM superfamily. *Crit. Rev. Biochem. Mol. Biol.* **43**, 63–88 (2008).
21. Chatterjee, A. *et al.* Reconstitution of ThiC in thiamine pyrimidine biosynthesis expands the radical SAM superfamily. *Nature Chem. Biol.* **4**, 758–765 (2008).
22. McGlynn, S. E. *et al.* Identification and characterization of a novel member of the radical AdoMet enzyme superfamily and implications for the biosynthesis of the Hmd hydrogenase active site cofactor. *J. Bacteriol.* **192**, 595–598 (2010).
23. Zhang, Y. *et al.* Diphthamide biosynthesis requires an organic radical generated by iron-sulphur enzyme. *Nature* **465**, 891–896 (2010).
24. Parast, C. V., Wong, K. K., Lewis, S. A. & Kozarich, J. W. Hydrogen exchange of the glycol radical of pyruvate formate-lyase is catalyzed by cysteine 419. *Biochemistry* **34**, 2393–2399 (1995).
25. Buis, J. M. & Broderick, J. B. Pyruvate formate-lyase activating enzyme: elucidation of a novel mechanism for glycol radical formation. *Arch. Biochem. Biophys.* **433**, 288–296 (2005).
26. Thauer, R. K. & Shima, S. Methane as fuel for anaerobic microorganisms. *Ann. NY Acad. Sci.* **1125**, 158–170 (2008).

Supplementary Information is linked to the online version of the paper at [www.nature.com/nature](http://www.nature.com/nature).

**Acknowledgements** We thank D. Barondeau and his laboratory for use of the anaerobic chamber and for advice on the assembly of Fe-S clusters in radical SAM enzymes. We also thank C. Xu for help with some of the <sup>31</sup>P NMR spectra and S. Burrows for help with cloning *phnI* and *phnH*. This work was supported in part by the National Institutes of Health (GM93342, GM71790) and the Robert A. Welch Foundation (A-840). The cryoprobe for the NMR spectrometer was purchased with funds from the National Science Foundation (0840464).

**Author Contributions** S.S.K., H.J.W. and F.M.R. designed the experiments. S.S.K. and H.J.W. performed the experiments. S.S.K., H.J.W. and F.M.R. wrote the manuscript.

**Author Information** Reprints and permissions information is available at [www.nature.com/reprints](http://www.nature.com/reprints). The authors declare no competing financial interests. Readers are welcome to comment on the online version of this article at [www.nature.com/nature](http://www.nature.com/nature). Correspondence and requests for materials should be addressed to F.M.R. (raushel@tamuedu).